Walk Distance Estimation Using an Ankle-mounted Inertial Measurement Unit

Helder D. Silva, *Member, IAENG*, Jose A. Afonso, *Member, IAENG*, and Luis A. Rocha

Abstract—**This work proposes walk distance estimation methods suitable for low power, low computational capability devices, using an ankle-mounted inertial measurement unit. A stride detection method using gyroscope data was implemented, and two stride length estimation methods were developed using the stride cycle information: a simple method, which estimates the leg angle during the forward swing of the leg; and an improved method, which uses the inverted pendulum model to provide the initial conditions for integration of the gyroscope and accelerometer signals in the three-dimensional space. The proposed methods were compared with a two-dimensional stride length estimation method, highlighting the importance of misalignments during sensor placement. Compared to the two-dimensional method, the simple method proposed in this paper achieved approximately the same level of performance with lower computational costs, whereas the three-dimensional method achieved 67% to 78% improvement in performance.**

Index Terms—**Walk Distance; Stride Detection; Stride Length Estimation; Inertial Measurement Unit; Low Computational Capability.**

I. Introduction

WITH the popularization of activity tracking devices such as Fitbit [1], stride (or step) detection (SD) and stride length (SL) estimation features are increasingly ubiquitous nowadays, featured not only in dedicated devices, but also in smartphones and smartwatches. The quality of the SD/SL estimation is an issue associated with these devices [2], which often place the inertial sensors in the waist [3], wrist [4], hand or pocket. Since this information is generally used to estimate burnt calories, its accuracy is typically overlooked. However, in the case of positioning systems, where a pedestrian dead-reckoning system uses these features to track the whereabouts of the user, accuracy is very important.

A pedestrian dead reckoning system uses an inertial measurement unit (IMU) to detect patterns in the accelerometer/gyroscope data in order to explore the human gait cycle [5]. During steady walking, all the states from both the stance and swing phases of the gait cycle are clearly identified in the IMU data. Some states can be missing from the data stream under specific conditions [6], such as walking in uneven terrain, climbing stairs, walking uphill or downhill [7]. Another cause for missing states from the gait cycle is related to health [8] or disability issues of the user [9]. For a healthy person, when the stride ends in the mid-swing, the heel-strike state can be absent from the measurements, causing estimation errors.

A robust solution for stride detection is the placement of the IMU on the foot, which enables accurate detection of inactivity periods, allowing the application of zero-velocity updates to correct drift errors. These updates provide the initial conditions for the integration of accelerations during a single stride (i.e., integration is reset every stride and gravity is removed from the accelerations), achieving errors in the order of 0.3% to 3% of total travelled distance [10]–[13]. Another strategy is to apply a model or an empirical formula to the IMU data during one stride [14], [15], resulting in errors between 3% to 8% of total travelled distance.

When the device is placed in the ankle or shank, the same methodology of zero-velocity update is applied. Solutions such as [16], [17] only consider movements in the sagittal plane, and assume that the sensor is perfectly vertical during the vertical event, thus providing the initial conditions for the integration of the acceleration. However, a tilt angle in the inertial sensor during the vertical event causes errors in the removal of gravity, thus influencing the SL estimation. The misalignment of the device can be seen as a common issue when placing the IMU in the ankle; therefore, robustness against misalignment conditions is desirable in a real use-case scenario.

The aim of this work is to robustly detect strides and estimate stride length by placing the device in a specific position and orientation, so the body axes of the gyroscope are (at least) coarsely aligned with the global vertical and forward axes. Following an approach based on [16], and taking in consideration that the algorithms are to be applied to devices with low computational capabilities, SL estimation is implemented in this work by placing the IMU on the user's ankle. This work addresses the misalignment problem by applying a quaternion-based orientation estimate in order to remove the gravity acceleration from the double integration process.

II. Methods

A. Stride Detection

When placing the sensor node on the user's ankle, the x-axis (forward direction axis) of the IMU is aligned with the direction of movement. The rotations in the sagittal plane are

Manuscript received January 17, 2017. This work was supported by FCT with the reference project UID/EEA/04436/2013, COMPETE 2020 with the code POCI-01-0145-FEDER-006941. Helder D. Silva was supported by FCT under the grant SFRBD/78018/2011.

Helder D. Silva is with CMEMS-UMinho, University of Minho, Campus of Azurem, Guimaraes, 4800-058, Portugal (phone: +351-253510190; fax: +351-253510189; e-mail: helderdavidms@gmail.com).

Jose A. Afonso is with CMEMS-UMinho, University of Minho, Campus of Azurem, Guimaraes, 4800-058, Portugal (e-mail: jose.afonso@dei.uminho.pt).

Luís A. Rocha is with CMEMS-UMinho, University of Minho, Campus of Azurem, Guimaraes, 4800-058, Portugal (e-mail: lrocha@dei.uminho.pt).

ISBN: 978-988-14047-4-9
ISSN: 2078-0958 (Print); ISSN: 2078-0966 (Online)

sensed mainly by the *y*-axis of the gyroscope, which is used in the algorithm to detect the phases of the gait cycle.

For every new measurement collected from the IMU, the main gyroscope axis is filtered using a second order Butterworth low pass filter with a cut-off frequency of 4 Hz (such as in [18]). This data is then used in the search for events by comparing the current and the previous filtered sample, with knowledge of the previous state of the gyroscope signal (e.g., rising or falling). A set of events is identifiable:

- A local maximum, when the gyroscope signal changes the slope from positive to negative;
- A zero crossing, when the gyroscope signal changes sign;
- A local minimum when the gyroscope signal changes the slope from negative to positive;
- A combination of both local maximum followed by a zero crossing and local minimum followed by a zero crossing.

Whenever an event is detected, it is used to update the finite state machine (FSM) depicted in Figure 1.

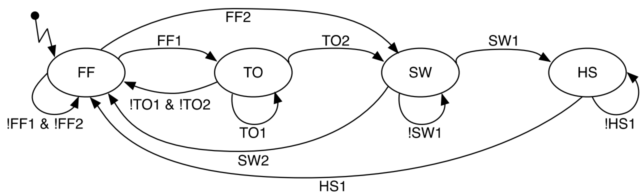

Fig. 1. Stride detection algorithm finite state machine.

The symbols "!" and "&" in the transitions between states in the FSM represent the logical operations NOT and AND, respectively. The FSM starts in the foot-flat (FF) state, where it searches for the local maximum event. When this event is detected and the previous filtered sample is higher than the predefined threshold, the transition to the toe-off (TO) state occurs. By using a threshold, part of the false positive local maximum events that would trigger a transition to the toe-off state are discarded. The FSM can also transit to the swing (SW) state directly if the local maximum followed by zero-crossing event occurs (e.g., due to a slow update rate or faster stride speed).

Occasionally, in the toe-off state, multiple local maximum events can occur, either due to walking in irregular pavements or due to slow walking. As such, the FSM stays in the toe-off state if this event is found. The transition from toe-off state to the swing state occurs when the zero crossing event is detected; otherwise, the FSM goes to the initial state to start searching for the local maximum event again.

After entering the swing state, the FSM searches for a zero crossing event, which typically appears immediately before the heel-strike (HS). When this event is found, a stride is evaluated. A stride is considered valid only when the maximum absolute value of the current filtered sample during the swing state was higher than the threshold. This threshold is less rigid than the typical thresholds applied in other methods, since the decision of SD does not solely depend on this minimum threshold value. The conditions for each state transition of the FSM are described as follows:

- FF1: the event is a local maximum and the previous filtered value is higher than the threshold;
- FF2: the event is local maximum followed by zero crossing and the previous filtered value is higher than the threshold;
- TO1: the event is local maximum;
- TO2: the event is zero crossing;
- SW1: the event is zero crossing or local minimum followed by zero crossing and the stride is valid;
- SW2: the event is zero crossing and the stride is invalid;
- HS1: the event is local maximum or local maximum followed by zero crossing.

The stride detection method proposed in this work is compared to the methods implemented in [19] and [20], which apply threshold algorithms to the accelerometer and gyroscope signals respectively. Although applied to the foot, these algorithms can also be used when the IMU is placed in the ankle. Both algorithms apply a low pass filter to the signals of interest before processing. The authors in [20] do not clearly state what type of filter is used, as such, a median filter was applied.

B. Stride Length Estimation

Two methods were implemented for SL estimation in this work:

- A simple method, with lower computation complexity, which integrates the angular velocity from the gyroscope during the interval when the user swings the leg forward;
- An improved method, with higher computation complexity, based on the algorithm applied in [16], where the integration of the ankle acceleration is performed during individual gait cycles.

A pendulum model, presented in Figure 2, is used as an approximation model to the simple SL estimation method.

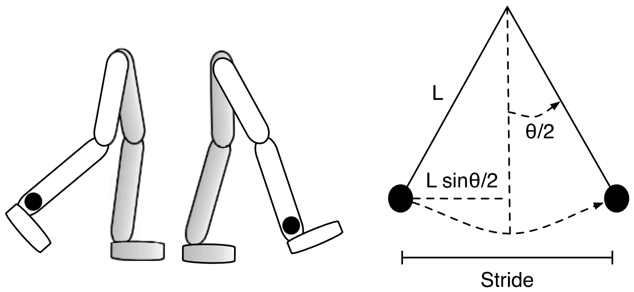

Fig. 2. Pendulum model approximation for stride length estimation.

This model depends on the user's leg length, found by applying the method used in [21], which measures the distance between the medial malleolus and the anterior superior iliac spine. Assuming that the angle described by the forward swing of the leg (from the toe-off until the heel-strike) is proportional to the stride, the arc length estimates the stride length, given by:

$$SL_1 = 2 \cdot L \cdot \sin\left(\frac{\theta}{2}\right), \quad (1)$$

where L is the leg length in meters and θ is the angle in radians. In order to avoid trigonometric calculations, equation (2), which calculates the length of the arc described

ISBN: 978-988-14047-4-9
ISSN: 2078-0958 (Print); ISSN: 2078-0966 (Online)

by the ankle motion, may be used as an approximation to the SL, instead of equation (1).

$$SL_2 = L \cdot \theta. \tag{2}$$

The angle θ is computed by integrating the raw gyroscope measurements from all axes.

When the user performs a turn while walking, a bias can also appear in the SL estimation, since the integration is accounting for movements outside the main sagittal plane. However, turning while walking does not occur often, since people tend to walk in straight paths. This bias in SL is generally small and can be disregarded due to its low frequency during walking.

For the improved method, the algorithm from [16] is applied, using the ankle vertical event. When this event is detected, the angle of the IMU with the vertical axis is assumed as zero. This provides the initial condition for the integration of the gyroscope data using equation (3), starting from the quaternion identity (i.e., quaternion vector [1, **0**]):

$${}^b_w q_i = {}^b_w q_{i-1} + \frac{1}{2} {}^b_w q_{i-1} \otimes \omega \cdot \Delta t, \tag{3}$$

where ${}^b_w q_{i-1}$ is the previous iteration of the gyroscope-based quaternion rotation from body frame (b) to world frame (w). The x, y and z axes form a right-handed coordinate system and point in the north, west and up directions respectively. Rotations for roll, pitch and yaw angles are given by the right-hand rule (thumb pointing in the axis direction while remaining fingers give the rotation direction). The symbol $\otimes$ denotes the quaternion multiplication, $\boldsymbol{\omega}$ is a quaternion with zero scalar part and vector part equal to the filtered angular velocity sample from the gyroscope (in rad/s), and Δt is the sampling period. The world frame acceleration is computed using equation (4):

$${}^w a = {}^b_w q_i \otimes {}^b a \otimes {}^b_w q_i^*, \tag{4}$$

where ${}^b a$ is the filtered acceleration sample in the body frame, obtained from sampling the IMU, and ${}^b_w q_i$ is the quaternion conjugate of the current orientation estimate. The acceleration in world frame is given by the vector part of quaternion ${}^w a$. The effect of gravity is present in this acceleration. In [16], it is removed by simply subtracting gravity (9.81 m/s^2) from the vertical axis. However, since the zero-angle in the ankle vertical event is an approximation, it is not guaranteed that the gravity vector is precisely vertical with respect to the body frame. The gravity vector depends on: misalignments during the placement of the IMU; the anatomy of the user's leg, which might not allow a perfectly vertical position for the IMU; as well as the user's posture during the FSM's ankle vertical event when walking. Therefore, instead of using the assumed vertical axis from the world frame, the filtered body frame acceleration sampled during the ankle vertical event is used as an approximation to the gravity vector, in order to account for a possible tilt angle, which would otherwise influence the removal of gravity for the duration of the step. The integration and final correction of the stride length are performed using equations (5) and (6), with initial values set to zero:

$${}^w v = \int_0^T \left({}^w a - {}^w a_g \right) \cdot dt + {}^w v(0), \tag{5}$$

$${}^w s = \int_0^T {}^w v \cdot dt - \frac{1}{2} T \cdot {}^w v(T). \tag{6}$$

The results from the simple and the improved stride length estimation methods are compared in section III.B to the method used in [16].

C. *Experimental Methods*

The sensor node uses a CC2530 system-on-chip connected to a MPU-6000 (IMU), which integrates an accelerometer and a gyroscope sensor. The sensor node collects measurements from the IMU at a frequency of 100 Hz. The gyroscope and accelerometer dynamic ranges were set to 1000 °/s and 4 g, respectively, guaranteeing that no sensor output saturation occurred and the signals of interest remained well within range, in order to avoid non-linear behaviors.

Sensor calibration was performed on site. Minimum and maximum values were found for the accelerometer by manually aligning the sensing axis with the direction of gravity. The gyroscope bias was found by averaging the samples while the sensor is static. Scale factor calibration of the gyroscope was also carried out by performing multiple 360-degree rotations in each axis while manually adjusting the scale factor, in order to obtain 0-degree angle when the sensor returns to the original orientation. Temperature calibration was not performed. In order to reduce the temperature effect, the sensor was powered on for several minutes prior to data collection, so a working temperature could be achieved.

All data collection was performed after an informed consent was received from the volunteers. Two subjects were asked to perform a specific set of routes under normal and fast walking paces. The sensor node was attached to the right ankle in the lateral side using a Velcro strap. Three routes were planned for the subjects to follow:

- A straight path where the subject walks from one point to the other and back, without making any turn while walking (route 1);
- A path around a Hall, which includes turns (route 2);
- A path that includes turns, stairs and irregular pavements (route 3).

The route distances were measured using a distance-measuring wheel, for which the distances of 127.6, 42.05 and 136.1 meters were measured for routes 1, 2 and 3, respectively.

Lengths of 82 cm and 86 cm were measured for the legs of subject A and B, respectively, using a measuring tape, according to the method used in [21]. Equation (2) is used for the simple SL estimation method. The improved method filters the IMU signals with a 2nd order Butterworth filter with a cut-off frequency of 4 Hz. The distances derived from the SL estimation methods were compared to the true measured distances.

The users counted the number of strides taken from start to finish while performing each route, in order to estimate

ISBN: 978-988-14047-4-9
ISSN: 2078-0958 (Print); ISSN: 2078-0966 (Online)

the SD error. The proposed SD algorithm is applied with the threshold parameter configured to 50 °/s, a value that was found empirically during the algorithm trials. The threshold effectively constrains how small or slow is the stride that the algorithm can detect. A value of 50 °/s is well below the typical angular velocity during slow walking.

III. Results

A. Stride Detection

A sample of the states identified by the SD algorithm implemented in this work is presented in Figure 3.

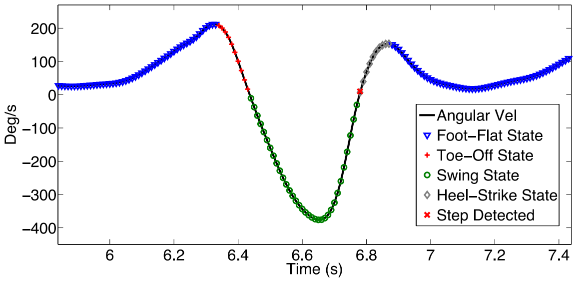

Fig. 3. State identification of the stride detection algorithm during the gait cycle.

The toe-off state is detected when the local maximum event is observed for a value of angular velocity above the threshold. This is followed by a rapid decrease in angular velocity, which happens during the forward leg swing. During this state, the FSM searches for a zero crossing event. When this event is found, a stride is evaluated by verifying if the minimum value of the filtered gyroscope axis is greater in absolute value than the threshold. The verification of this condition, along with the zero-crossing event, triggers the transition to the heel-strike state, which signals the SD event.

The results for the routes performed by subject A and B are presented in Table I. The stride detection algorithm successfully detected all strides for subject A and overestimated a total of four strides for subject B. These false positive detections occurred during turns in the fast pace trials of subject B. The stride detection algorithm implemented in this work outperformed the other algorithms in all trials.

B. Walk Distance Estimation

The proposed methods provide improvements and tradeoffs in the SL estimation. The results for subject A and B are summarized in Table II.

The simple method performed approximately at the same level of the other more complex algorithms in the normal pace trials. For the faster pace, this method consistently underestimated the SL. The overall error percentage for the simple method is comparable to the method in [16], which uses an higher computation complexity algorithm.

The improved method achieved overall lower error percentage, exhibiting improvements of 78% and 67% for users A and B, respectively, compared to the method in [16].

IV. Discussion

This work presented a simple and accurate stride detection method, based on a finite state machine and the segmentation of the gait cycle. The SD method provided the basis for the stride length estimation, in order to infer walk distance.

The influence of misalignments that can occur due to the placement of the device, posture or anatomical characteristics of the user was identified and compensated. The importance of these misalignments was demonstrated in the improved SL estimation method by comparing the performance of the method used in [16] to the solution proposed in this work. The misalignments were addressed in the improved method, which resolved the accelerations in three-dimensions and estimated the initial tilt of the IMU during the ankle vertical event.

By attaching the node to the ankle, some minor disturbances were expected due to the leg muscles that are activated during specific instants of the gait cycle. By applying a low pass filter to the signal of interest, these disturbances were greatly attenuated and did not influence the SL.

Subject B, although not very different than subject A in terms of leg length, exhibited a faster pace in both trials. This faster pace can explain the lower accuracy results from subject B compared to subject A, due to the underestimation of the SL under these conditions.

In the case of the simple SL estimation method, a consistent underestimation was observed in the faster pace trials. One possible explanation for this is due to a greater contribution to the SL from the supporting foot during mid-swing. Since the gyroscope cannot detect this contribution, the SL has a tendency to be underestimated. By using equation (2), the SL is overestimated by default, which counters the supporting foot contribution. In the case of equation (1), the underestimation of the SL would be

TABLE I
Stride Detection Count and Error Percentage Results for Subjects A and B

Route	True Count		SD Algorithm		Jimenez [19]		Feliz [20]	
	A	B	A	B	A	B	A	B
Route 1 Normal	106	105	106 0%	105 0%	107 0.9%	106 0.9%	109 2.8%	112 2.8%
Route 1 Fast	84	80	84 0%	80 0%	84 0%	81 1.3%	86 2.4%	82 2.5%
Route 2 Normal	33	33	33 0%	33 0%	33 0%	33 0%	37 12.1%	34 3.0%
Route 2 Fast	29	27	29 0%	28 3.7%	29 0%	30 11.1%	33 13.8%	29 7.4%
Route 3 Normal	101	98	101 0%	98 0%	102 1.0%	101 3.1%	111 9.9%	109 11.2%
Route 3 Fast	94	88	94 0%	91 3.4%	91 3.2%	77 12.5%	95 1.1%	94 6.8%
Σ |Error|	0	0	0 0%	4 0.9%	5 1.1%	19 4.4%	24 5.4%	29 6.7%

ISBN: 978-988-14047-4-9
ISSN: 2078-0958 (Print); ISSN: 2078-0966 (Online)

TABLE II
WALK DISTANCE ERROR IN METERS AND ERROR AS A PERCENTAGE OF TOTAL TRAVELLED DISTANCE FOR SUBJECTS A AND B

Route	Simple Method		Improved Method		Li [16]	
	A	B	A	B	A	B
Route 1	2.93	1.09	-0.66	2.79	-6.82	-16.40
Normal	2.3%	0.9%	-0.5%	2.2%	-5.3%	-12.9%
Route 1	-11.11	-13.09	1.11	7.27	-5.22	-11.39
Fast	-8.7%	-10.3%	0.87%	5.7%	-4.1%	-8.9%
Route 2	0.22	-0.71	0.40	1.19	-1.51	-4.72
Normal	0.5%	-1.7%	1.0%	2.8%	-3.6%	-11.2%
Route 2	-2.48	-3.27	0.53	1.24	-1.51	-4.09
Fast	-5.9%	-7.8%	1.3%	2.9%	-3.6%	-9.7%
Route 3	-9.01	-10.77	-1.02	5.42	-7.84	-14.40
Normal	-6.6%	-7.9%	-0.7%	4.0%	-5.8%	-10.6%
Route 3	-15.32	-17.97	-3.84	4.72	-11.78	-16.7
Fast	-11.3%	-13.2%	-2.8%	3.5%	-8.7%	-12.3%
Σ |Error|	41.07	46.90	7.56	22.63	34.68	67.74
	6.7%	7.7%	1.2%	3.7%	5.7%	11.1%

greater, which would result in higher percentage of error. The use of equation (2) compensates this effect and also unburdens the sensor node from trigonometric calculations.

When using the simple SL method, the leg length parameter becomes an important scaling factor in determining the correct SL. This requires the user to measure and configure this parameter correctly. The method from [21] provided a precise measure of the leg length, producing consistent results in terms of total travelled distance. Further data collection and analysis is necessary to confirm the accuracy of this approach across a bigger sample of users.

REFERENCES

[1] J. Takacs, C. L. Pollock, J. R. Guenther, M. Bahar, C. Napier, and M. A. Hunt, “Validation of the Fitbit One activity monitor device during treadmill walking,” *J. Sci. Med. Sport*, vol. 17, no. 5, pp. 496–500, 2014.

[2] A. Sushames, A. Edwards, F. Thompson, R. McDermott, and K. Gebel, “Validity and Reliability of Fitbit Flex for Step Count, Moderate to Vigorous Physical Activity and Activity Energy Expenditure,” *PLoS One*, vol. 11, no. 9, pp. 1–14, 2016.

[3] F. A. Storm, C. Buckley, and C. Mazzà, “Gait event detection in indoor and outdoor settings: Accuracy of two inertial sensors based methods,” *Gait & Posture*, vol. 50, pp. 42–46, 2016.

[4] C. Tudor-Locke, T. V. Barreira, and J. M. Schuna, “Comparison of step outputs for waist and wrist accelerometer attachment sites,” *Med. Sci. Sports Exerc.*, vol. 47, no. 4, pp. 839–842, 2015.

[5] R. Harle, “A Survey of Indoor Inertial Positioning Systems for Pedestrians,” *IEEE Commun. Surv. Tutorials*, vol. 15, no. 3, pp. 1281–1293, Jan. 2013.

[6] S. K. Park and Y. S. Suh, “A zero velocity detection algorithm using inertial sensors for pedestrian navigation systems.,” *Sensors (Basel).*, vol. 10, no. 10, pp. 9163–78, Jan. 2010.

[7] Q. Ladetto, “On foot navigation : continuous step calibration using both complementary recursive prediction and adaptive Kalman filtering,” *ION GPS*, pp. 1735–1740, Sep. 2000.

[8] P. Newland, J. M. Wagner, A. Salter, F. P. Thomas, M. Skubic, and M. Rantz, “Exploring the feasibility and acceptability of sensor monitoring of gait and falls in the homes of persons with multiple sclerosis,” *Gait & Posture*, vol. 49, pp. 277–282, 2016.

[9] O. Suciu, R. R. Onofrei, A. D. Totorean, S. C. Suciu, and E. C. Amaricai, “Gait analysis and functional outcomes after twelve-week rehabilitation in patients with surgically treated ankle fractures,” *Gait & Posture*, vol. 49, pp. 184–189, 2016.

[10] A. R. Jiménez, F. Seco, J. C. Prieto, and J. Guevara, “Indoor pedestrian navigation using an INS/EKF framework for yaw drift reduction and a foot-mounted IMU,” in *2010 7th Workshop on Positioning, Navigation and Communication*, 2010, pp. 135–143.

[11] X. Yun, J. Calusdian, E. R. Bachmann, and R. B. McGhee, “Estimation of Human Foot Motion During Normal Walking Using Inertial and Magnetic Sensor Measurements,” *IEEE Trans. Instrum. Meas.*, vol. 61, no. 7, pp. 2059–2072, Jul. 2012.

[12] E. Foxlin, “Pedestrian tracking with shoe-mounted inertial sensors,” *IEEE Comput. Graph. Appl.*, vol. 25, no. 6, pp. 38–46, 2005.

[13] I. Skog, P. Händel, J.-O. Nilsson, and J. Rantakokko, “Zero-velocity detection - An Algorithm Evaluation,” *IEEE Trans. Biomed. Eng.*, vol. 57, no. 11, pp. 2657–2666, 2010.

[14] H. Weinberg, “Using the ADXL202 in pedometer and personal navigation applications,” Application Note AN-602, Analog Devices, 2002.

[15] J. W. Kim, H. J. Jang, D.-H. Hwang, and C. Park, “A Step, Stride and Heading Determination for the Pedestrian Navigation System,” *J. Glob. Position. Syst.*, vol. 3, no. 1&2, pp. 273–279, Dec. 2004.

[16] Q. Li, M. Young, V. Naing, and J. M. Donelan, “Walking speed estimation using a shank-mounted inertial measurement unit,” *J. Biomech.*, vol. 43, no. 8, pp. 1640–1643, 2010.

[17] B. Sijobert, M. Benoussaad, J. Denys, R. Pissard-Gibollet, C. Geny, and C. Azevedo Coste, “Implementation and Validation of a Stride Length Estimation Algorithm, Using a Single Basic Inertial Sensor on Healthy Subjects and Patients Suffering from Parkinson’s Disease,” *Health (Irvine. Calif).*, vol. 7, pp. 704–714, June 2015.

[18] Q. Li, M. Young, V. Naing, and J. M. Donelan, “Walking speed and slope estimation using shank-mounted inertial measurement units,” in *2009 IEEE International Conference on Rehabilitation Robotics*, 2009, pp. 839–844.

[19] A. R. Jimenez, F. Seco, C. Prieto, and J. Guevara, “A comparison of Pedestrian Dead-Reckoning algorithms using a low-cost MEMS IMU,” in *2009 IEEE International Symposium on Intelligent Signal Processing*, 2009, pp. 37–42.

[20] R. Feliz, E. Zalama, and J. G. García-Bermejo, “Pedestrian tracking using inertial sensors,” *J. Phys. Agents*, vol. 3, no. 1, pp. 35–42, 2009.

[21] P. P. Gogia and J. H. Braatz, “Validity and reliability of leg length measurements.,” *J. Orthop. Sports Phys. Ther.*, vol. 8, no. 4, pp. 185–8, 1986.